UNIVERSIDAD DEL ISTMO
www.unistmo.edu.mx

"2020, AÑO DE LA PLURICULTURALIDAD DE LOS PUEBLOS INDÍGENAS Y AFROMEXICANO"

OFICIO No. 065/DGA/UNISTMO/2020
Asunto: *Gastos De publicación, Solicitud de Liberación.*
Sto. Domingo Tehuantepec, Oax., 19 de noviembre de 2020

Lic. Lorenzo Manuel Loera de la Rosa
Director de Superación Académica

AT´N:
Lic. Graciela Hernández Sánchez
Subdirectora de Análisis y Evaluación Docente

Por este conducto le envío un cordial saludo, al tiempo que remito la **Solicitud de Liberación** correspondiente al *apoyo para Gastos de Publicación* autorizado al **PTC RICARDO CARREÑO AGUILERA**, adscrito a la Universidad del Istmo. Cabe señalar que el apoyo fue autorizado mediante oficio No. 511-6/2020-3091, de fecha 23 de marzo de 2020.

Nombre del PTC	*Revista / ISSN*	*Título del artículo*	*Costo (M.N.)*
Dr. Ricardo Carreño Aguilera	Fractals / 0218-348X	PARAMETER ESTIMATION SPACE FOR UNKNOWN INTERNALEVOLUTION ON IOT-DOMOTIC SYSTEMS	$25,000.00

Se adjunta solicitud de liberación por parte del PTC en comento, Informe final (impacto académico logrado), copia del artículo publicado; y desglose financiero de recursos que emite la Universidad del Istmo. Los documentos en PDF se enviaron al correo victorh.osornio@nube.sep.gob.mx.

Garantizando la transparencia en el ejercicio de los recursos, agradezco la atención prestada al presente, y aprovecho la ocasión para agradecer los apoyos que nos brinda el Programa en mejora de la educación de nuestra región, nuestro estado y por ende nuestro país.

ATENTAMENTE

Voluntas totum potest
Guiraa zanda ne guendaracala'dxi'

L.C.E. Claudia Hernández Cela
Jefa del Departamento de Gestión Académica

UNIVERSIDAD DEL ISTMO
PROGRAMA PARA EL DESARROLLO PROFESIONAL DOCENTE, PARA EL TIPO SUPERIOR
PRODEP
REPRESENTANTE INSTITUCIONAL

C.f.p .-Dr. Modesto Seara Vázquez.- Rector de la Universidad del Istmo.- Para su conocimiento.
.-Dr. Israel Flores Sandoval.- Vice-rector Académico.- Universidad del Istmo.- Mismo fin.
.-Dr. Ricardo Carreño Aguilera.- Profesor-Investigador.- Universidad del Istmo.- para seguimiento.
.- Archivo
*CHC/

Sto. Domingo Tehuantepec Oaxaca a 02 de noviembre de 2020

Asunto: Gastos de publicación,
Solicitud de Carta de Liberación.

Lic. Lorenzo Manuel Loera de la Rosa
Director de Superación Académica

AT´N: Lic. Graciela Hernández Sánchez
Subdirectora de Análisis y Evaluación Docente

Sirva el presente para enviarle un cordial saludo y mi agradecimiento por el apoyo recibido en el proyecto Gastos de Publicación. Así mismo, aprovecho la ocasión para solicitarle de la manera más respetuosa la **Carta de Liberación** correspondiente al apoyo recibido en mérito del Programa, autorizado en el oficio No. 511-6/2020-3091 de fecha 23 marzo del 2020. Es importante comentar que el artículo titulado "parameter stimation space for unknown internal evolution on IOT domotic systems", se publicó en la revista fractals, con ISSN 0218-348, en el volumen 28-3 de fecha 16 marzo del 2020.

Se adjunta al presente, copia del artículo publicado en revista indexada, así como, informe final que contiene el impacto académico logrado con el apoyo recibido.

Sin más por el momento quedo de usted.

ATENTAMENTE.

"Voluntas totum potest"
Guirá' zanda ne guendaracala'dxi'

Dr. Ricardo Carreño Aguilera
NOMBRE Y FIRMA DEL PROFESOR-INVESTIGADOR

C.c.p. –Dr. Israel Flores Sandoval.- Vice-rector Académico.- Universidad del Istmo.-Para su conocimiento.
.-L.C.E. Claudia Hernández Cela.- Representante Institucional ante el Programa.- Universidad del Istmo.-Mismo fin.
.-Archivo

Universidad del Istmo

INFORME FINAL

GASTOS DE PUBLICACIÓN

IES de adscripción:	**Universidad del Istmo**	**Título de la publicación:**	parameter estimation space for unknown internal evolution on IOT domotic systems
Nombre del PTC:	**Dr. Ricardo Carreño Aguilera**	**Nombre de la Revista:**	Fractals Journal….
ID del PTC:	**UNISTMO-172804**	**ISSN:**	0218-348
Número de oficio de autorización:	511-6/2020-3091	**Link: (opcional)**	https://www.worldscientific.com/doi/10.1142/S0218348X20500668
Fecha de autorización:	**23 marzo del 2020**	**Monto aprobado**	$25,000

Impacto académico logrado con el apoyo recibido:

Ejemplo: El artículo publicado hasta el momento del presente informe ha tenido 86 descargas y es una revista JCR de factor de impacto 4.5……………………………………………………………………

Dr. Ricardo Carreño Aguilera
Profesor-Investigador

L.C.E. Claudia Hernández Cela
Representante Institucional ante PRODEP

UNISTMO

UNIVERSIDAD DEL ISTMO

prodep
TIPO SUPERIOR

PROGRAMA PARA EL DESARROLLO PROFESIONAL DOCENTE, PARA EL TIPO SUPERIOR 2020
OFICIO APROBACION DSA 511-6/2020-3091 07'MAR'2020
GASTOS DE PUBLICACIÓN

Beneficiario : RICARDO CARREÑO AGUILERA

Fecha	No. Ch. / T.E.	No. Comprobante	Beneficiario del Pago	R.F.C.	Concepto del Gasto	IMPORTE FACTURA (Ejercido)	GASTOS DE PUBLICACIÓN
			Monto Aprobado				**$ 25,000.00**
04/06/2020	13089	6120/DGA/2020	REVISTA " FRACTALS JOURNAL" ISSN 0218-348X	***	PAGO DEL ARTICULO " PARAMETER ESTIMATION SPACE FOR UNKNOWN INTERNAL EVOLUTION ON IOT DOMOTIC SYSTEMS"	$ 25,000.00	$ -
					Total Gastos	**$ 25,000.00**	**$ -**

Cd. Ixtepec, Oax. a 15 de Junio 2020

L.C. Yazmín Carolina López Morales
Jefa del Departamento de Recursos Financieros

UNISTMO DEPARTAMENTO DE RECURSOS FINANCIEROS

L.C.E Eugenio Cortés Hernández
Vice-Rector de Administración

UNISTMO VICE-RECTORIA DE ADMINISTRACION

Fractals, Vol. 28, No. 3 (2020) 2050066 (9 pages)

DOI: 10.1142/S0218348X20500668

PARAMETER ESTIMATION SPACE FOR UNKNOWN INTERNAL EVOLUTION ON IOT DOMOTIC SYSTEMS

R. CARREÑO AGUILERA*
Universidad del Istmo, Cd. Universitaria S/N, 70760
Tehuantepec, Oaxaca, México
ricardo.carreno.a@hotmail.com

J.J. MEDEL JUAREZ
Instituto Politécnico Nacional, CIC
México City, México

S. L. GOMEZ CORONEL
Instituto Politécnico Nacional, UPIITA
México City, México

Received August 9, 2019
Accepted February 27, 2020
Published March 16, 2020

Abstract

This paper describes the parameter estimation modeling concerning a domotic designer bot system with internet of things (IoT) assistance using the probabilistic operator based on the stochastic parameter estimation through the moments and the recursive conditions. Light, CCTV, presence, and temperature are IoT data monitored, shared, and accessed by the internet for a smart office designer performance that evolves based on historical web data. The relationship established by Wiener between covariance and variance found the parameter time evolution by observing through the time. The development is viewed in the visible results between non-recursive and recursive mathematical structures. In both cases, the convergence rate is based on probabilistic estimation, the functional error presents a high convergence rate which is viewed as an effect of the function of a density function. The estimate considered a non-invasive perspective, and it helps in different applications such as health diagnosis in

*Corresponding author.

humans and animals with internal problems, or systems which are unknown for internal evolution such as for IoT model adoption. Therefore, our objective is to propose a black box, inner approximation through the parameter estimation without a no invasive stochastic method based in Wiener approximation.

Keywords: Pattern Recognition; IoT (Internet of Things); Parameter Estimation; Identification of Variables; Recursive Filters.

1. INTRODUCTION

Estimating parameters allows us to see the stability of the fractal itself and define its characteristics unlike what we have so far seen of fractals. Besides, estimating the parameters of a system allows us to get an intrinsic view of the system, something that is not obtained in conventional fractal modeling which only considers the dimension and its structure. Some studies have been done for internet of things (IoT) domotic system stability using Lyapunov stability. However, in this case, the stability study is done with an estimation parameter space considering the IoT domotic system as a fractal behavior system. The main contribution of this paper is to find a mathematical model to facilitate the stability study for IoT domotic systems considering these systems as a fractal behavior. This study was chosen in the IoT systems due to a near boom on IoT after the 5G internet mass adoption.

The stochastic recursive filter is possible now due to mathematical and computational advances.[1,2]

The scientific advances in the two last centuries put solid, durable bases into senses, deterministic and stochastic systems.

With these premises, it gives the tools required for probabilistic recursive stochastic parameter estimation applied to the unknown internal evolution system.

Therefore, the first concept used was an internal product of the two stochastic variables developed by the German mathematician, David Hilbert (1862–1943). The second was of the German mathematician, Johann Carl Frederic Gauss (1777–1855), and his Gaussian probabilistic distribution function or normal function.

Both concepts are used for determining the moment second of a stochastic system, and a third concept was used for a Martingales concept introduced by France, Paul Levy (1886–1971), to perform the graphical evaluation.

The Maximum Entropy method is applied, which is a system based on LaGrange multipliers to determine an appropriate probabilistic distribution to choose the representative model of the black-box process, in which there is previous experimental information of its input/output variables.

2. RECURSIVE BLACK-BOX MODEL

The model' purpose is to determine the stochastic parameter estimation in two steps: first, the error functions called co-variance Pk, Qk, and second,[3] their recursive forms.[4,5] These errors are obtained using the Gaussian distribution density probabilistic function.[6]

2.1. Characteristics of the Black Box

The study process is a black-box model with a single-input and single-output (SISO) with the following features: linear and time-invariant with adhered noise to the internal state and output. It can be seen in Eqs. (1) and (2) (ARMA model).[7–9]

The Autoregressive-Moving Average (ARMA) model is a well-researched forecasting tool that provides good quality short-term forecasts on stationary, non-seasonal time-series.

$$\tilde{x}_{k+1} = a\tilde{x}_k + b\tilde{w}_k, \tag{1}$$

$$\tilde{y}_k = c\tilde{x}_k + d\tilde{v}_k, \tag{2}$$

where $x_k \epsilon R^n, y_k \epsilon R^p$ are the internal and output variables and $w_k \epsilon R^l$, $v_k \epsilon R^p$ are noises with mean value equal to zero being stationary with a white noise process with correlation.

2.2. Recursive Process

The space state Eqs. (1) and (2) help us to build the ARMA model in a recursive form,[10,11] where the noise is now a combination thereof and added to the output system, see the following equations:

$$\hat{y}_k = \hat{y}_{k-1} + \hat{V}m_k, \tag{3}$$

$$\hat{V}m_k = -ad\tilde{v}_{k-1} + d\tilde{w}_{k-1} + b\tilde{w}_{k-1}. \tag{4}$$

2.3. Internal Product of Hilbert

This method consists of multiplying y_{k-1} with the recursive response, see the following equation:

$$\hat{y}_k\hat{y}_{k-1} = a\hat{y}_{k-1}^2 + \hat{V}m_k\hat{y}_{k-1}. \tag{5}$$

2.4. Stochastic Estimation

The stochastic operators used to perform the parameter estimation $\tilde{a}$ are mean value, variance, and covariance.[12–19]

Applying the mathematical expectation to Eq. (5) and estimate the parameter a, we have the following equations:

$$E\{\hat{y}_k\hat{y}_{k-1}\} = aE\{\hat{y}_{k-1}^2\} + E\{\hat{V}m_k\hat{y}_{k-1}\}, \tag{6}$$

$$E\{\hat{y}_k\hat{y}_{k-1}\} = aE\{\hat{y}_{k-1}^2\} - adE\{\tilde{v}_{k-1}\hat{y}_{k-1}\}, \tag{7}$$

$$\tilde{a}_k = \frac{E\{\hat{y}_k\hat{y}_{k-1}\}}{E\{\hat{y}_{k-1}^2\} - dE\{\tilde{v}_{k-1}\hat{y}_{k-1}\}}. \tag{8}$$

2.5. Discrete Probabilistic Mean Value

The discrete probabilistic mean value applied to a discrete random variable[20,21] $\tilde{y}_i$ is shown in the following equation:

$$E\{\hat{y}_i\} = \sum_{i=1}^{k} \hat{y}_i P_Y(Y \leq \hat{y}_i), \tag{9}$$

where Y is a random variable sequence, and P_Y is the probabilistic dummy function of y_i.

2.6. Accumulated Probabilistic Density Nonlinear Function

Nonlinear systems such as seismic and DNA genome alignment,[22,23] and also recognition and machine learning systems,[24–28] but in this case, IoT systems[29] observe unknown internal evolution processes. These types of systems can define the accumulated probabilistic density function $dF_Y(\hat{y}_i)/d\hat{y}_i$ or distribution function $F_{y_i}(y_i)$ and has the following form of the equations:

$$F_Y(\hat{y}_i) = P_Y(Y \leq \hat{y}_i), \tag{10}$$

$$P_Y(\tilde{y}_i) = \frac{dF_Y(\hat{y}_i)}{d\hat{y}_i}. \tag{11}$$

Otherwise, the density function of the probability of the random variable Y is the derivative of the probability density accumulated function.

If Eq. (11) expresses the finite differences

$$P_{Y(t)|_{Y(t-\varepsilon)}},(\hat{y}_i) \cong \frac{F(\hat{y}_i) - F(\hat{y}_{i-\varepsilon})}{\varepsilon}, \tag{12}$$

where ϵ is equal to the digital interval k samples and of one value. Therefore, Eq. (12) comes to be the following equation:

$$P_Y(\hat{y}_i) \cong F(\hat{y}_i) - F(\hat{y}_{i-1}). \tag{13}$$

According to the definition in Eq. (10), it has the following equation:

$$P_Y(\hat{y}_i) \cong P(\hat{y}_i) - P(\hat{y}_{i-1}). \tag{14}$$

2.7. Probability Density Nonlinear Function (pdf)

A random variable Y has a Gaussian or a dummy variable $\tilde{y}_i$ expressed in the following equation:

$$P_Y(\hat{y}_i) = \frac{1}{\sigma_Y\sqrt{2\pi}} e^{\left(-\frac{(\hat{y}_i-\mu_Y)^2}{2\sigma_Y^2}\right)}. \tag{15}$$

2.8. Maximum Entropy

It gives us the most appropriate distribution to the model described in Eqs. (1) and (2), particularly the one with the highest entropy among all those that satisfy the constraints of our prior black-box system knowledge. Usually, these constraints are equations regarding moments of the desired distributions. Besides, the system has the most significant remaining uncertainty, and by observing its bias, do not we add any correlated noise into the estimation.

Applying the maximum entropy description, considering that it has two signals (the output system signal and the identification signal), we seek to accomplish Eq. (16).

$$\delta\left[-k\sum_{i=1}^{y} P_Y(y_i)\ln(P_Y(y_i)) - \alpha\sum_{i=1}^{y} P_Y(\hat{y}_i)\right] \cong 0. \tag{16}$$

Despite the innovation properties that the output system signal had, and based on maximum entropy property, probabilities between identification and reference converge in almost all points, i.e. $P_Y(\hat{y}_i) \sim P_Y(y_i)$, which allows us to select the variances and mean values as a part of the estimation and identification with respect random variable Y.

Using the Taylor series, the exponential function expressed by a convergent sequence is as follows:

$$e^{-a} = \sum_{n=1}^{\infty} \frac{(-1)a^n}{n!} \cong 1 - a. \tag{17}$$

Then exponential function based on the previous result reduces to a difference as in the following equation:

$$e^{-a} - e^{-b} = b - a. \tag{18}$$

The probabilistic density function of the random variable Y is

$$P_Y(\hat{y}_i) = \frac{1}{\sqrt{8\pi\sigma_Y^3}}(y_i^2 - y_{i-1}^2 - 2\mu_Y(y_i - y_{i-1})). \tag{19}$$

The random variable second-order moment in discrete has the following form:

$$E\{\hat{y}_i^2\} = \sum_{i=1}^{k} y_i^2 P_Y(Y \leq y_i). \tag{20}$$

The correlation function allows using the second probability moment, but in the expanded description as

$$E\{\hat{y}_k \hat{y}_{k-1}\} = \sum_{i=1}^{k} (y_k y_{k-1}) P_Y(Y \leq y_i). \tag{21}$$

By substituting the result of Eq. (19) into Eq. (21) we have the covariance error function P_k in the following equation:

$$P_k = E\{\hat{y}_k \hat{y}_{k-1}\} = \frac{1}{\sqrt{8\pi\sigma_Y^3}} \sum_{i=1}^{k} (y_i y_{i-1})(y_i^2 - y_{i-1}^2 - 2\mu_Y(y_i - y_{i-1})). \tag{22}$$

By performing operations we obtain the digital sequence of covariance error in the following equation:

$$P_k = \frac{1}{\sqrt{8\pi\sigma_Y^3}}(\hat{y}_k^3 \hat{y}_{k-1} - \hat{y}_k \hat{y}_{k-1}^3 - 2\mu(\hat{y}_k^2 \hat{y}_{k-1} - \hat{y}_k \hat{y}_{k-1}^2) + P_{k-1}. \tag{23}$$

In the same sense, the covariance error using the variance and the innovation moment has the following form of equation:

$$Q_k = E\{\hat{y}_{k-1}^2\} - dE\{\tilde{v}_{k-1}\hat{y}_{k-1}\}. \tag{24}$$

In this case, there are two moments, one square of the output variable and the other, to the same output variable and the output noise as in the following equation:

$$Q_K = \frac{1}{\sqrt{8\pi\sigma_Y^3}} \sum_{i=1}^{k} (\hat{y}_{i-1}^2 - d\tilde{v}_{i-1}\hat{y}_{i-1})(\hat{y}_i^2 - \hat{y}_{i-1}^2 - 2\mu_Y(\hat{y}_i - \hat{y}_{i-1})). \tag{25}$$

We develop it as a sequence that is dependent on sampling: the output variable, output noise, and the parameters of the Gaussian probability density function σ and μ. See the following equation:

$$\begin{aligned} Q_K = \frac{1}{\sqrt{8\pi\sigma_Y^3}} (&\hat{y}_{k-1}^2 \hat{y}_k^2 - \hat{y}_{k-1}^4 - 2\mu_Y(\hat{y}_k \hat{y}_{k-1}^2 - \hat{y}_{k-1}^3) \\ &- d\tilde{v}_{k-1}\hat{y}_{k-1}\hat{y}_k^2 + d\tilde{v}_{k-1}\hat{y}_{k-1}\hat{y}_k^3 \\ &+ 2\mu_Y(\tilde{dv}_{k-1}\hat{y}_{k-1}\hat{y}_k - d\tilde{v}_{k-1}\hat{y}_{k-1}^2)) + Q_{k-1}). \end{aligned} \tag{26}$$

With the two sequences P_k and Q_k, the Wiener standard description in the recursive form concerning $\hat{\hat{a}}$ has the following equation:

$$\hat{\hat{a}} = \frac{\frac{1}{\sqrt{8\pi\sigma_Y^3}} \begin{pmatrix} \hat{y}_k^3 \hat{y}_{k-1} - \\ \hat{y}_k \hat{y}_{k-1}^3 - \\ 2\mu(\hat{y}_k^2 \hat{y}_{k-1} - \\ \hat{y}_k \hat{y}_{k-1}^2 \end{pmatrix} + P_{k-1}}{Q_k}. \tag{27}$$

In order to enable the equation to obtain the covariance function Q_k and not of P_k, we use a delay on the comparison and proceed to substitute P_{k-1} by $Q_{k-1}a_{k-1}$, see Eq. (28). We finish with the new discrete estimation algorithm of stochastic parameters applied to a black box.

Equation (27), based on covariance Q_k and not P_k, delays and proceeds to replace P_{k-1} by $Q_{k-1}a_{k-1}$. See Eq. (28) and finishing with a new stochastic discrete parameter algorithm applied to a black box.

$$\hat{a}_k = \left(\frac{Q_{k-1}}{Q_k}\right)\hat{a}_{k-1} + \left(\frac{1}{\sqrt{8\pi\sigma_Y^3}}\right)\rho_k. \tag{28}$$

3. FUNCTIONAL ERROR

Mathematical expressions commonly used determine the non-recursive functional error considering the discrete probabilistic mathematical expectation in Eq. (29), and recursive form for stable conditions in (30).

Non-recursive

$$\tilde{e}_k = a_k - \tilde{a}_k, \tag{29}$$

$$\tilde{J}_k = \left(\frac{1}{k}\right) \sum_{i=1}^{n} \tilde{e}_i^2. \tag{30}$$

Recursive

Based on (29) with stationary conditions through time evolution error, we have the following equation:

$$\hat{J}_k = \left(\frac{1}{k}\right) (\hat{e}_k^2 + (k-1)\hat{J}_{k-1}). \tag{31}$$

In the interpretation of the IoT domotic designer models, the Hough probabilistic transform is used by the Hough Lines P function.

4. EXPERIMENTAL RESULTS

4.1. Parameters and Initial Conditions

In what follows, we give some data that are carried out to make the simulation for domotic IoT expert systems.[29–31]

```
a=0.9;                     % PROCESS
b=1.3;                     % PROCESS
c=1.5;                     % PROCESS
d=0.3;                     % PROCESS
%------------------------------------------
SIGMA=1.9.0;             % (VARIANCE)
MU=11.2;                 % (MEAN VALUE)
%------------------------------------------
%INITIAL CONDITIONS
%------------------------------------------
x(1)=0.8;                 % STATES OF PROCESS
yn(1)=0.12;               % OUTPUT OF PROCESS
%------------------------------------------
pp(1)=0.00009;          % ERROR OF COVARIANCE
qp(1)=0.0008;             % ERROR OF COVARIACE
%------------------------------------------
anp(1)=0.11;              %P.E. NO RECURRENTE
amrp(1)=0.33;                % P.E. RECURRENT
er(1)=0.004;            % NON RECURRENT E. E.
J(1)=0.005;             % NON RECURRENT E. E.
erp(1)=0.006;               % RECURRENT E. E.
J1(1)=0.003;                     % RECURRENT
```

4.2. Non-Recursive Validation

The graph presents the comparative digital algorithm solutions found in Secs. 2 and 3. Non-recursive (NR) and recursive (R) solutions are shown in blue. For the following initial conditions, the validation using graphs showed the simulation comparing the non-recursive solution (blue) with the recursive (red) one.

Figure 1 shows the stochastic output response (NR) related to Eq. (2) and (R) Eq. (3). The figure is simulated for clearance of 100 samples. There is an overshoot of 0.15 (after 10 events) of amplitude and then managed to tune to an amplitude of 0.01 on a continuous form. The non-recursive (NR) and recursive (R) are confusing in the ten samples.

Figure 2 presents a histogram determining some essential characteristics in the data of non-recursive (NR) and recursive (R) output variables, where,

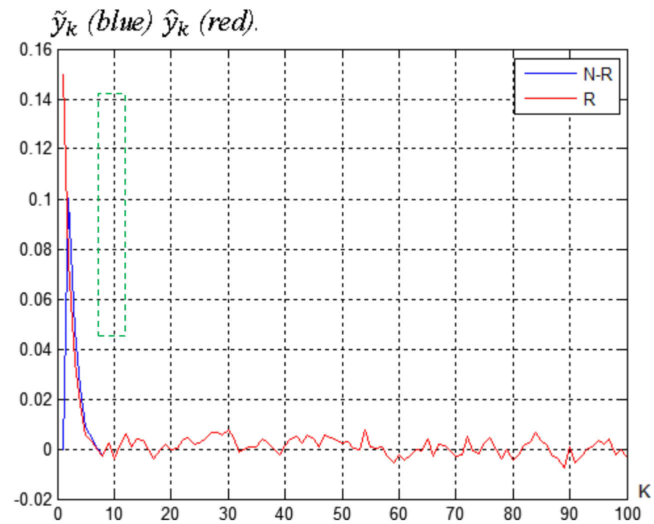

Fig. 1 Stochastic output variable $\tilde{y}_k$ (blue) and recursive identification $\hat{y}_k$ (red).

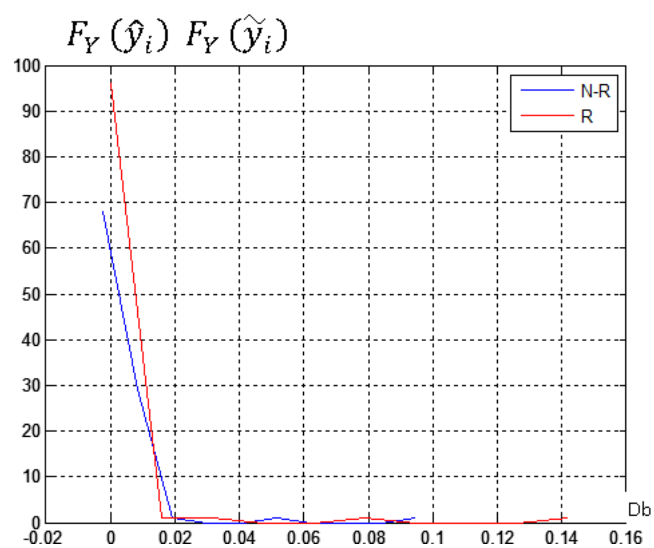

Fig. 2 Histogram of the stochastic output variable $\tilde{y}_k$ (Blue) and recursive stochastic output variable $\hat{y}_k$ (red).

both systems focused on having the data in the output black-box variable (red) in the center, reach a higher frequency, and compare with the non-recursive (blue).

Figure 3 shows the case of the graphic of the functional error, the two responses achieve confused state, totally around 0.0001 of stabilization, thus this precision is obtained.

In Fig. 4, the graph of recursive stochastic parameter estimated shows the fit the non-recursive stochastic parameter estimate absolutely without appreciable error. It is also adjustable in the region of stability in the range $0 < \hat{\hat{a}} < 1$. Figure 4

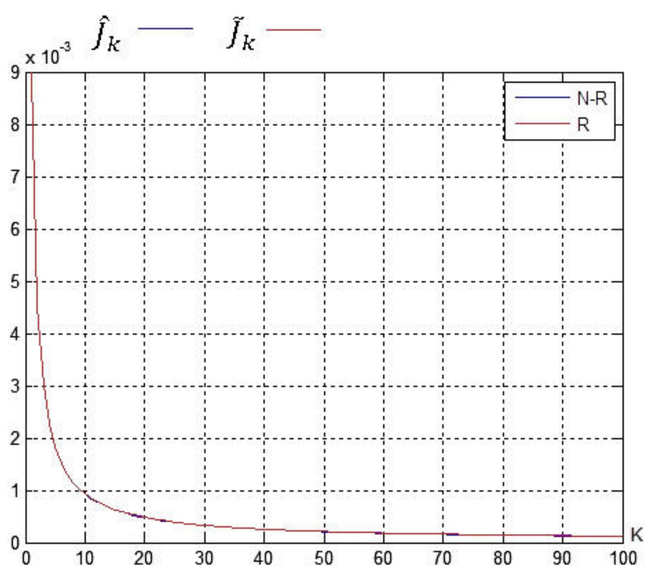

Fig. 3 Functional error in recursive form $\tilde{J}_k$ (blue) and non-recursive $\hat{J}_k$ (red).
Note: Both are confused in one.

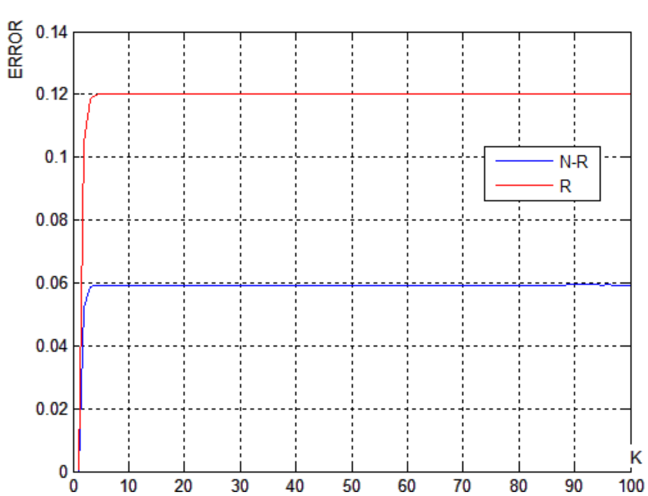

Fig. 4 Stochastic parameter process 0.5, estimated recursive parameter $\tilde{a}$ (blue) and estimated recursive probabilistic parameter $\hat{a}_k$ (red), obtaining confused by only one (red).

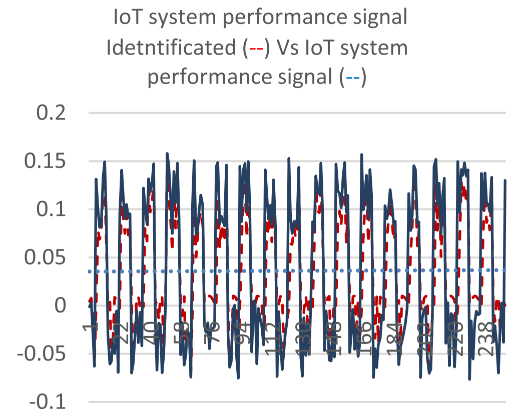

Fig. 5 Identification and the Domotic IOT reference signal.

presented a process with an estimated value of 0.5. With this value, a steady balance is achieved without wavering.

Simulation in Fig. 5 shows that the data output of both stochastic variables reaches approximately the same amplitude in decibels and cuts in a 0.02 dB amplitude. Besides, it has a slight bias.

We consider a stochastic synthetic NLTV signal created from the interval function given in Eq. (16), which has variations in frequency, amplitude, with $\{\xi\_k\} \subseteq N(\mu, \sigma \wedge 2 < \infty)$, an average value.

The cumulative systematic error e_k, represented by the second probability moment through the functional $J\_k(e\_k) = E\{e\_k \wedge 2\}$ is useful to measure the convergence level. This error is determined point-to-point, at instant k, through the difference between reference and the respective identification in each case. The domotic IoT model considered in (31) shows brain activity.

$$y_k = 0.02\,k\,0.50\sin(0.014\pi k) + 0.8\,\xi_k, \quad 0 < k \leq 250. \tag{32}$$

The graph in Fig. 6 shows different values of the non-recursive and recursive parameters estimated for $0 < \hat{\hat{a}} < 1$.

In Fig. 6, observe that most of the values are moving between the range 0 to -0.3 except by the 0.3 spike observed, which represents a steady behavior.

The absolute mean error is shown in Fig. 7 (MAE, Mean Absolute Error). In these tests values 4.8 mm, 8.9 mm and 2.2 mm were for the x, y and z axes, respectively. Among the causes of the systematic errors observed are those related to the transformation of coordinates and the derivatives of operations (median, dilation and Hough transform) performed to determine the pairs of parallel lines.

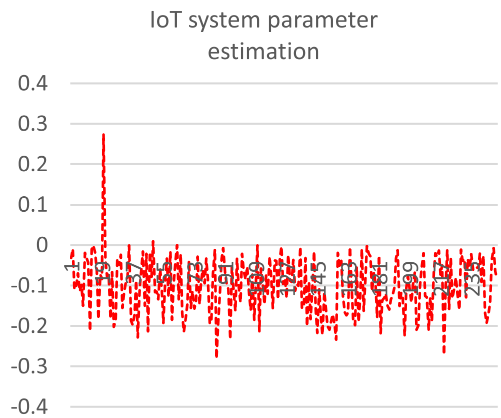

Fig. 6 Domotic IoT process parameter estimation.

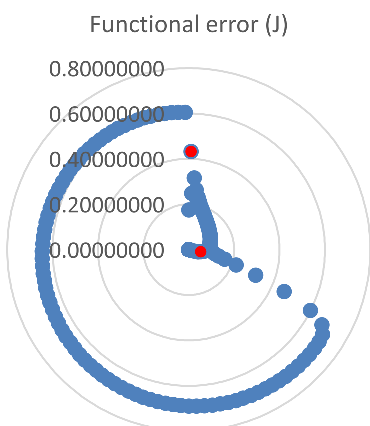

Fig. 7 Domotic IoT system functional error.

By using the Canny filter and the Hough transform, it was observed that these methods could be more efficient when using images in which larger objects exist. However, the limitations of the space did not allow the use of larger objects.

As shown in Fig. 8, the ESS designs are delivered by the Bot_designer software after the coordinate is taken to the bot by the user.

The bot, which is the software human interface of the expert system, can design a layout for office areas. In Fig. 8, we see an example with a lobby area (the area with a receptionist), the cubicle areas (the areas with small desks for employees), and the meeting room (the space for meetings), all of them for the first floor in this case. Note that the vortices of the construction are C1–C8, which are two-dimensional coordinates $(X,\ Y)$ given by the user of the bot. S1–S4 are three-dimensional coordinates $(X,\ Y,\ Z)$, which represent the location of the sensors (temperature, lighting, presence, camera, etc.) for this smart office. The actual readings of the sensors are sent to the internet and the sensors can be

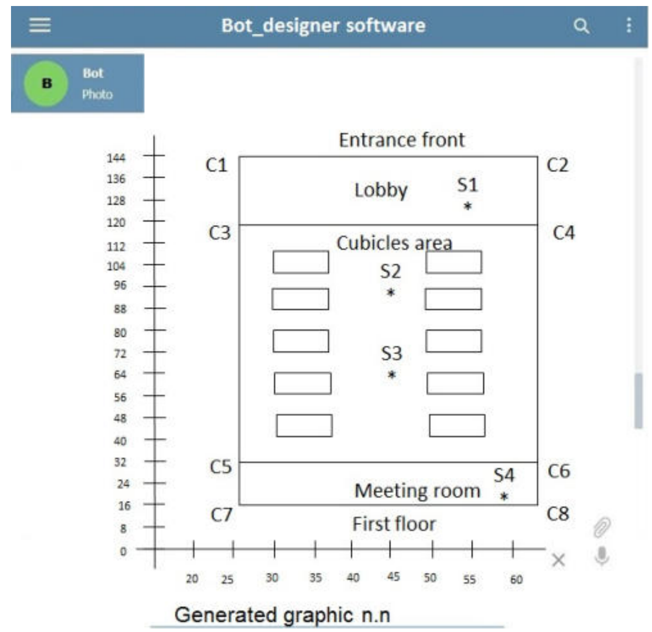

Fig. 8 Expert system service (ESS) design.

controlled by a remote device. By creating, in this way, an IoT layout with a domotic office, the IoT system is not the core of this paper, but the bot designer is the core.

5. DISCUSSION

Parameter estimation with probabilistic space for an IoT-domotic drawing designer expert system is the core objective of this paper, which can be a designer for any number of drawings and schematics. The specific focus of this paper is domotic sensor installation drawings in smart building offices, but no less appealing than the combination between some innovative concepts such as in the neural network topic (The extreme learning machine). The purpose of combining these concepts is to be at the cuting edge of the state-of-the-art IoT domotic development. However, sometimes, the innovation cannot be a synonym of efficiency, this triad combination — designer bot, expert system, and extreme learning machine — will need to be optimized for scalability in a mass usage environment. Facilitating the optimization is the reason for the utility of a parameter estimation study for this kind of process. Also, note the potential of the designer expert system as the core for a drawing designing revolution.

Initial conditions were obtained stochastically, this means that the code starts running stochastically until observing the best results. Parameters and initial conditions in this paper are found under best fractal behavior result.

6. CONCLUSIONS

Our design achieves the no-recursive and recursive stochastic algorithm of parameter estimates using the moment second of Gaussian probability.

Stability on the IoT parameter estimation is obtained in the range of −0.3 to 0, as shown in Fig. 6, however, the most important thing about Fig. 6 is that stability is possible for IoT models shown as a fractal behavior, as discussed in this paper. In Fig. 6, a spike almost reaches a value of 0.3, which the represents chaos unwanted.

Figure 7 shows the findings of the simulation precisions in the level of thousandths for functional error. Thus, by trial and error, the stability of non-recursive and recursive stochastic parameters is estimated.

Parameter estimation probabilistic study can be applied to unknown internal evolution IoT-Domotic systems since function error can tend to a limit as a minimum, as shown in Fig. 7.

REFERENCES

1. M. Santiago, Las computadoras como herramientas de aprendizaje, *Griot.* **1**(6) (2018) 19–25.
2. P. M. Jacovkis, Computadoras, modelización matemática y ciencia experimental, *Rev. Iberoamericana de Ciencia, Tecnol. Soc.* **5**(2) (2005) 51–63.
3. E. A. Valencia and C. M. Escobar, El concepto de la esperanza condicional en las Martingalas. *Sci. Technica* **14**(39) (2008) 394–398.
4. K. Petersen, Ergodic theory: Basic examples and constructions, in *Mathematics of Complexity and Dynamical Systems*, 2011 edn. (Springer, USA, 2011).
5. M. Choda, Around Shannon's interpretation for entropy preserving stochastic averages, *Int. J. Math.* **25**(10) (2014) 1–10.
6. V. S. Pugachev, *Probability Theory and Mathematical Statistics for Engineers*, 1st edn. (Pergamon Press, Oxford, 1984).
7. W. Yu *et al.*, Modeling of gasoline blending via discrete time neural networks, *Neural Netw. Proc.* **2004** (2004) 6.
8. W. Yu *et al.*, Neural networks for the optimization of crude oil blending, *Int. J. Neural Syst.* **15**(5) (2005) 377–389.
9. R. Carreño *et al.*, Comparative analysis on nonlinear models for RON gasoline blending using neural networks, *Fractals* **25**(6) (2017) 1–8.
10. S. Lu *et al.*, Nonlinear autoregressive and nonlinear autoregressive moving average model parameter estimation by minimizing hypersurface distance, *IEEE Trans. Signal Process.* **51**(12) (2003) 3020–3026.
11. L. Sheng and J. Hwan, A new algorithm for linear and nonlinear ARMA model parameter estimation using affine geometry, *IEEE Trans. Biomed. Eng.* **48**(10) (2001) 1116–1124.
12. R. Carreño *et al.*, A nonlinear acoustic transducer model with variable structure control, *Fractals* **25**(2) (2017) 1–6.
13. S. Rionero, Lyapunov functionals for the coincidence between the first and the second Lyapunov stability methods, *New Trends in Fluid and Solid Models*, 1st edn. (World Scientific, Italy, 2009), pp. 113–121.
14. G. Bartolini, A. Ferrara and E. Usani, Chattering avoidance by second-order sliding mode control, *IEEE Trans. Autom. Control* **43**(2) (1998) 241–246.
15. V. I. Utkin, *Sliding Models in Control and Optimization*, 1st edn. (Springer-Verlag, Berlin, 1992), pp. 1–302.
16. W. Ming-Chin and S. Ming-Chang, Simulated and experimental study of hydraulic anti-lock braking system using sliding-mode PWM control, *Mechatronics* **13**(4) (2003) 331–351.
17. M. Bouri and D. Thomasset, Sliding control of an electropneumatic actuator using an integral switching surface, *IEEE Trans. Control Syst. Technol.* **9**(2) (2001) 368–375.
18. K. Ang, G. Chong and L. Yun, PID control system analysis, design, and technology, *IEEE Trans. Control Syst. Technol.* **13**(4) (2005) 559–576.
19. A. Girin, F. Plestan, X. Brun and A. Glumineau, High-order sliding-mode controllers of an electropneumatic actuator: Application to an aeronautic benchmark, *IEEE Trans. Control Syst. Technol.* **17**(3) (2009) 633–645.
20. R. Carreño *et al.*, Sliding mode control applied to a mini-aircraft pitch position model, *Comput. Sistemas* **18**(2) (2014) 409–416.
21. W. Yu and X. Li, Automated nonlinear system modeling with multiple fuzzy neural networks and kernel smoothing, *Int. J. Neural Syst.* **20**(5) (2010) 429–435.
22. J. Patiño *et al.*, Seismic activity seen through evolution of the Hurst exponent model in 3D, *Fractals* **24**(4) (2016) 1–10.
23. D. Pacheco *et al.*, Nonlinear FM index application for alignment of short DNA sequences using reparametrization of algorithms, *Fractals* **26**(3) (2018) 1–11.
24. M. E Acevedo *et al.*, Computational intelligence for shoeprint recognition, *Fractals* **27**(4) (2019) 1–13.
25. J. J. Carrasco, ELM regularized method for classification problems, *Int. J. Artif. Intell. Tools* **25**(1) (2016) 1–12.
26. G. B. Huang, What are extreme learning machines? Filling the gap between Frank Rosenblatt's dream

and John von Neumann's puzzle, *Cogn. Comput.* **7**(3) (2015) 263–278.
27. Y. Li, Extreme learning machine for determining signed efficiency measure from data, International Journal of Uncertainty, *Fuzz. Knowl. Based Syst.* **21**(2) (2013) 131–142.
28. H. T. Huynh *et al.*, An improvement of extreme learning machine for compact single-hidden-layer feedforward neural networks, *Int. J. Neural Syst.* **18**(5) (2008) 433–441.
29. R. Carreño *et al.*, An IoT expert system shell in block-chain technology with elm as inference engine, *Int. J. Inf. Technol. Decis. Making* **18**(1) (2019) 87–104.
30. W. Gu *et al.*, Expert system for Ice hockey game prediction: Data mining with human judgment, *Int. J. Inf. Technol. Decis. Making* **15**(4) (2016) 763–789.
31. C. A Magni *et al.*, An alternative approach to firms' evaluation: Expert systems and fuzzy logic, *Int. J. Inf. Technol. Decis. Making* **5**(1) (2016) 195–225.